Journal of Alloys and Compounds 480 (2009) 360–364

Contents lists available at ScienceDirect

Journal of Alloys and Compounds

journal homepage: www.elsevier.com/locate/jallcom

Phase equilibria in the quasi-ternary system Ag_2S–In_2S_3–CdS at 870 K

V.R. Kozer[a,*], A. Fedorchuk[b], I.D. Olekseyuk[a], O.V. Parasyuk[a]

[a] Department of General and Inorganic Chemistry, Volyn National University, Voli Ave. 13, 43025 Lutsk, Ukraine
[b] Department of Inorganic Chemistry, Lviv National University, Kyryla and Mefodiya St. 6, 79005 Lviv, Ukraine

ARTICLE INFO

Article history:
Received 8 April 2008
Received in revised form 12 February 2009
Accepted 13 February 2009
Available online 27 February 2009

Keywords:
Semiconductors
Chemical synthesis
X-ray diffraction

ABSTRACT

An isothermal section of the quasi-ternary system Ag_2S–CdS–In_2S_3 at 870 K was investigated using X-ray phase analysis. No quaternary intermediate phase was found. A continuous solid solution series between In_2S_3, $AgIn_5S_8$ and $CdIn_2S_4$ was discovered; a limited solid solution range of CdS is localized along the $AgInS_2$–CdS section.

1. Introduction

The crystal structure of adamantane semiconductors is characterized by the tetrahedral coordination of atoms which allows for the formation of solid solution range of substantial extents. The variations of the compositions of the solid solutions permit a wide range of the control of the properties thus leading to new possibilities of the optimization of the parameters of semiconductor devices.

An isothermal section of the quasi-ternary system Ag_2S–CdS–In_2S_3 had not been studied in detail until now, and no information was found in literature on the existence of intermediate quaternary phases in the system. Various authors [1–3] studied only the side sections Ag_2S–CdS, Ag_2S–In_2S_3, In_2S_3–CdS of the quasi-ternary system.

The Ag_2S–CdS is of the peritectic type [1] with the peritectic point coordinates 33 mol.% CdS and 1166 K. A horizontal line at 448 K is caused by the polymorphous transition of Ag_2S. A minor solid solubility based on Ag_2S extends to 4 mol.% CdS.

The latest investigation of the Ag_2S–In_2S_3 section was reported in [2]. The existence of the compounds $AgInS_2$ ($CuFeS_2$ structural type) and $AgIn_5S_8$ ($MgAl_2O_4$ structural type) was confirmed. The system liquidus consists of four regions of the primary crystallization of β-Ag_2S, β-$AgInS_2$, $AgIn_5S_8$, γ-In_2S_3. $AgInS_2$ forms incongruently at 1130 K. A solid solution range of Ag_2S extends to 8 mol.% In_2S_3 at 870 K. $AgIn_5S_8$ has a large homogeneity region from 81 to 100 mol.% In_2S_3 at 870 K as determined by the change of the unit cell parameters. The $AgIn_{11}S_{17}$ compound that was described in detail in [3] is in fact a part of this solid solution range. The continuous solid solution series is formed by the filling of the existing vacancies in the cation sub-lattice of the binary chalcogenide.

The In_2S_3–CdS section was investigated in [1]. The section is characterized by a continuous solid solubility between In_2S_3 and $CdIn_2S_4$. The existence of two ternary compounds, $CdIn_2S_4$ and $Cd_2In_2S_5$, was reported at the section. $CdIn_2S_4$ ($MgAl_2O_4$ structural type) melts congruently at 1398 K. $Cd_2In_2S_5$ forms in a solid-state reaction and decomposes above 1283 K; the compound is dimorphous (transition temperature is 1231 K).

The crystallochemical characteristics of the compounds of the Ag_2S–In_2S_3–CdS system at 870 K are presented in Table 1.

2. Experimental procedure

Phase equilibria of the Ag_2S–In_2S_3–CdS system were investigated using 119 samples. The batches were composed of high-purity metals and chalcogene (Ag: 99.99 wt%; Cd: 99.9999 wt%; In: 99.99 wt%; S: 99.997 wt%). First, the batches were heated in evacuated quartz containers in the oxygen-gas burner flame to complete bonding of elementary sulphur. The alloys were then synthesized by the single-temperature method in a shaft-type furnace. The maximum synthesis temperature was 1473 K with 5-h exposure. The alloys were annealed at 870 K during 1000 h followed by quenching into cold water. XRD spectra were recorded by DRON 4-13 diffractometer (CuKα radiation) in a step-scan mode ($10^\circ \leq 2\theta \leq 90^\circ$). The diffraction patterns were processed using CSD software package, the phase analysis utilized Powder Cell program [11].

3. Results

3.1. The In_2S_3–CdS section

The inconsistency of the literature data on the In_2S_3–CdS system led us to the re-investigation of this system. The section was studied

* Corresponding author. Tel.: +380 3322 49972; fax: +380 3322 41007.
E-mail address: kozer_v@mail.ru (V.R. Kozer).

0925-8388/$ – see front matter © 2009 Published by Elsevier B.V.
doi:10.1016/j.jallcom.2009.02.052

Table 1
The crystallochemical characteristics of the compounds of the Ag_2S–In_2S_3–CdS system at 870 K.

Compound	Space group (S.G.)	Unit cell parameters (nm)		References
		a	*c*	
β-Ag_2S	*Im*3*m*	0.4889	–	[5]
β-CdS	*P*6$_3$*mc*	0.4134	0.6749	[6]
β-In_2S_3	*Fd*3*m*	1.0774	–	[7]
α-$AgInS_2$	*I*42*d*	0.5879	1.1203	[8]
$AgIn_5S_8$	*Fd*3*m*	1.0828	–	[9]
$CdIn_2S_4$	*Fd*3*m*	1.0843	–	[10]

using 22 samples annealed at 870 K. The existence of the $CdIn_2S_4$ compound was confirmed, as well as its congruent melting and the crystal structure of the spinel type (S.G. $Fd\bar{3}m$). A new endothermal ternary compound of an approximate composition $Cd_5In_2S_8$ was discovered. The compound forms peritectically and has a polymorphous transition at 1265 K. The temperature range of the existence of $Cd_5In_2S_8$ is 1205–1390 K. The $B^{II}{}_5C^{III}{}_2X^{VI}{}_8$ compounds are not an exception of the In_2S_3–CdS system. An endothermal compound $Cd_5Ga_2S_8$ is known (the range of its existence is 1093–1238 K) [1]; in the systems HgSe–Ga_2Se_3 and HgSe–In_2Se_3, the ordering of the solid solutions occurs below 639 K at the compositions $Hg_5C^{III}{}_2Se_8$ [12].

We did not confirm the existence of $Cd_8In_2S_{11}$ and $Cd_2In_2S_5$ that were reported in [1,4]. The section CdS–$CdIn_2S_4$ was investigated by XRD of the samples annealed at 870 K and by DTA (Fig. 1). A horizontal line at 1265 K represents the polymorphous transition of $Cd_5In_2S_8$.

The isothermal section at 870 K contains a solid solution range of CdS (S.G. *P*6$_3$*mc*), a solid solution range of In_2S_3 and $CdIn_2S_4$

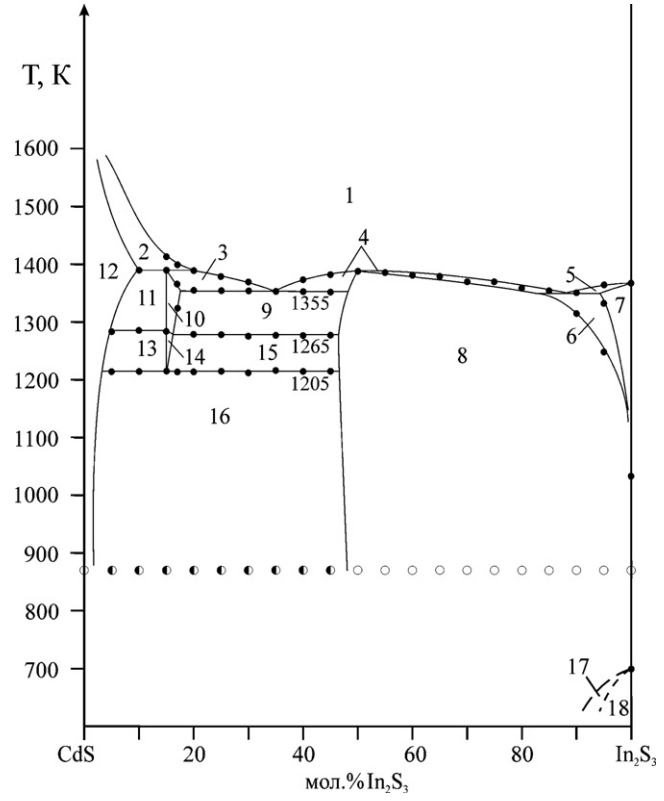

Fig. 1. Phase diagram of the CdS–In_2S_3 system: (1) L, (2) L+CdS, (3) L+β-$Cd_5In_2S_8$, (4) L+$CdIn_2S_4$, (5) L+γ-In_2S_3, (6) ε+γ-In_2S_3, (7) γ-In_2S_3, (8) ε, (9) β-$Cd_5In_2S_8$+$CdIn_2S_4$, (10) β-$Cd_5In_2S_8$, (11) β-$Cd_5In_2S_8$+CdS, (12) CdS, (13) α-$Cd_5In_2S_8$+CdS, (14) α-$Cd_5In_2S_8$, (15) α-$Cd_5In_2S_8$+$CdIn_2S_4$, (16) CdS+$CdIn_2S_4$, (17) α-In_2S_3+ε, (18) α-In_2S_3.

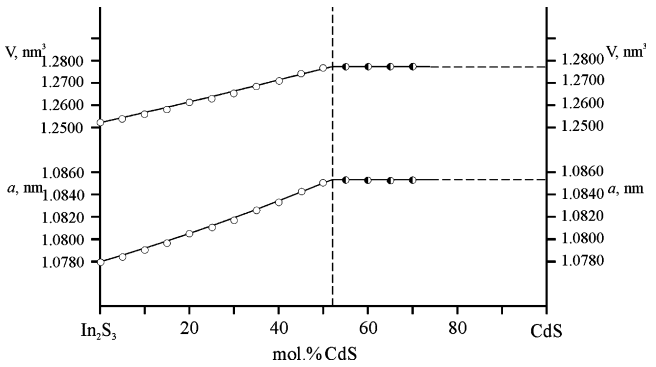

Fig. 2. The change of the unit cell parameters at the In_2S_3–$CdIn_2S_4$ section at 870 K.

with the cubic structure (S.G. *Fd*3*m*), and the two-phase region of their co-existence in the range 52–100 mol.% CdS. The alloys in the 0–52 mol.% CdS range are single-phase, and crystallize in the cubic structure of spinel.

The change of the unit cell parameters within the solid solution range is linear (Fig. 2); the *a* period and the volume of the cubic cell increase linearly with the $CdIn_2S_4$ content.

3.2. The $AgIn_5S_8$–$CdIn_2S_4$ section

Investigation of the $AgIn_5S_8$–$CdIn_2S_4$ section was performed on 11 samples. The phase diagram was constructed using XRD and DTA results (Fig. 3). The section belongs to Roozeboom Type I, with continuous miscibility in both solid and liquid state. The system below the solidus line forms a continuous α-solid solution series of the starting components. Due to the small difference of the melting points of both system components (~15 K), the liquidus and the solidus lines are nearly horizontal at the phase diagram; the thermograms recorded only one effect during heating and cooling cycle.

The change of the unit cell parameters of the investigated alloys is linear (Fig. 4). The *a* period and the cell volume increase linearly with the $CdIn_2S_4$ content. The mechanism of atom substitution in the crystal lattice of the solid solutions was additionally studied. The Wyckoff site 8a is occupied by the statistical mix In+Cd, the

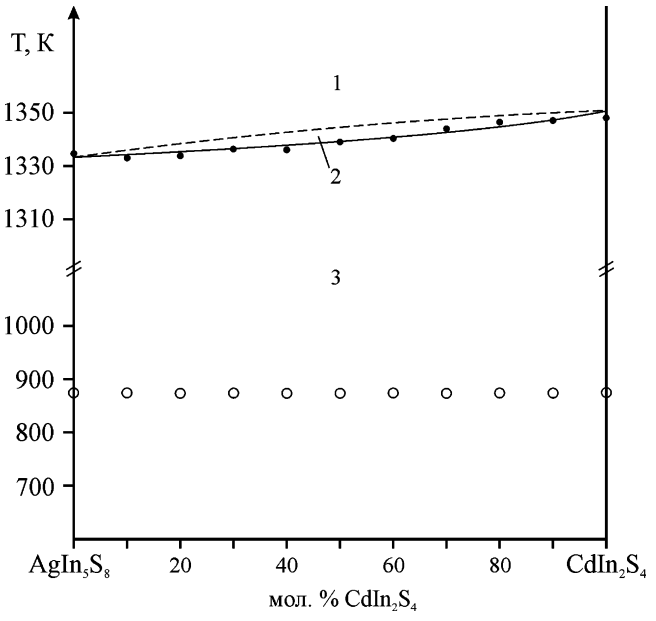

Fig. 3. Phase diagram of the $AgIn_5S_8$–CdIn2S4 system: (1) L, (2) L+α, and (3) α.

Table 2
Unit cell parameters for the solid solution with the spinel structure (S.G. $Fd\bar{3}m$).

mol.% $CdIn_2S_4$	0	20	40	50	60	80	100
16 CN 6	In	In	In	In	In	In	In
	$0.75 \times 0.94 = 0.705$	$0.78 \times 0.94 = 0.733$	$0.81 \times 0.94 = 0.761$	$0.83 \times 0.94 = 0.780$	$0.86 \times 0.94 = 0.808$	$0.92 \times 0.94 = 0.865$	$1.00 \times 0.94 = 0.940$
	Ag	Ag	Ag	Ag	Ag	Ag	
	$0.25 \times 1.29 = 0.323$	$0.22 \times 1.29 = 0.284$	$0.19 \times 1.29 = 0.245$	$0.17 \times 1.29 = 0.219$	$0.14 \times 1.29 = 0.181$	$0.08 \times 1.29 = 0.103$	
Mean radius	1.028	1.017	1.006	0.999	0.989	0.968	0.940
8 CN 4	In	In	In	In	In	In	Cd
	$1.00 \times 0.76 = 0.760$	$0.89 \times 0.76 = 0.676$	$0.75 \times 0.76 = 0.570$	$0.66 \times 0.76 = 0.502$	$0.57 \times 0.76 = 0.433$	$0.33 \times 0.76 = 0.251$	$1.00 \times 0.92 = 0.920$
		Cd	Cd	Cd	Cd	Cd	
		$0.11 \times 0.92 = 0.101$	$0.25 \times 0.92 = 0.230$	$0.33 \times 0.92 = 0.306$	$0.43 \times 0.92 = 0.396$	$0.66 \times 0.92 = 0.607$	
Mean radius	0.760	0.777	0.800	0.808	0.829	0.858	0.920
$\delta_{B\text{-}S}$	2.630(4)	2.628(3)	2.627(4)	2.623(5)	2.621(5)	2.618(4)	2.614(4)
$\delta_{A\text{-}S}$	2.484(4)	2.489 (3)	2.493(4)	2.501(5)	2.507(5)	2.512(4)	2.529(4)
a (nm)	1.0831(3)	1.0832(1)	1.0836(2)	1.0837(2)	1.0839(2)	1.0845(2)	1.0854(1)

16*d* site is occupied by Ag + In atoms, the 32*e* site is occupied by S atoms (Table 2). The occupation of all crystallographic sites was unity in the calculation model. Sulphur atoms are tetrahedrally coordinated; the coordination of the statistical mix is a tetrahedron as well, that of Ag + In atoms is an octahedron.

Using the ionic radii (which depend on the surrounding), we calculated the averaged radii of the elements in 8(a) and 16(d) sites. As shown in Table 2, the averaged radius in the 16(d) site decreases, while that in the 8(a) site increases. Presenting the structure as the packing of the layers formed of octahedra and tetrahedra along the body axis, the increase of the averaged radius of the element in the 8(a) site which forms tetrahedra leads simultaneously to the increase of the number of octahedra in this layer. Since octahedra in both layers are formed around the atoms of the same sort, the octahedral layers become thicker, thus the cell dimensions increase (Fig. 5).

Experimental diffraction patterns of the $AgIn_5S_8$–$CdIn_2S_4$ section are presented in Fig. 6.

3.3. XRD study of the $AgInS_2$–CdS section

XRD investigation of the $AgInS_2$–CdS system utilized 22 samples. The solid solubility based on low-temperature modification of $AgInS_2$ at 870 K is less than 2 mol.% CdS. The solid solution range of CdS at 870 K is 59–100 mol.% CdS (Fig. 7).

3.4. System $AgInS_2$-$CdIn_2S_4$

The $AgInS_2$–$CdIn_2S_4$ is non-quasi-binary both in the solid-state and in the liquidus region (Fig. 8). The section liquidus is represented by the single line of the primary crystallization of β-solid solutions. The two-phase field L + $AgIn_5S_8$ below the liquidus stretches across the entire section.

The section solidus is formed by the line of the plane of the invariant peritectic equilibrium at 1123 K. The peritectoid process reflects the polymorphous transition of $AgInS_2$.

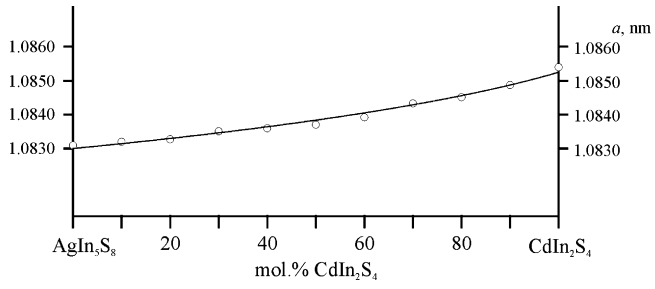

Fig. 4. The change of the unit cell parameters at the $AgIn_5S_8$–$CdIn_2S_4$ section at 870 K.

The section at the annealing temperature contains the following fields: single-phase regions of $AgInS_2$ and $CdIn_2S_4$, a two-phase region of $CdIn_2S_4$ + CdS, a three-phase region of β-$AgInS_2$ + HPTP + CdS.

The section features a minor solid solubility in LT-$AgInS_2$ that does not exceed 3 mol.% $CdIn_2S_4$. The solid solubility in $CdIn_2S_4$ is ~13 mol.% at the annealing temperature.

3.5. Isothermal section of the quasi-ternary system Ag_2S–In_2S_3–CdS

Based on the XRD results, an isothermal section of the quasi-ternary system Ag_2S–In_2S_3–CdS at 870 K was constructed. The chemical and phase composition of the alloys is plotted in Fig. 9. The section is characterized by large areas of single-phase and two-phase regions. The triangulating sections of the system at 870 K are $AgInS_2$–CdS and $AgIn_5S_8$–$CdIn_2S_4$. They separate the quasi-ternary system into 3 sub-systems.

The Ag_2S–$AgInS_2$–CdS sub-system features the equilibrium of α-, β- and γ-solid solutions. Similarly, the combination of three solid solutions (β, γ and ε) defines the phase equilibria in the $AgInS_2$–CdS–In_2S_3 sub-systems.

As $AgIn_5S_8$, In_2S_3 and $CdIn_2S_4$ are isostructural (S.G. $Fd3m$), this leads to the mutual solid solubility of all three compo-

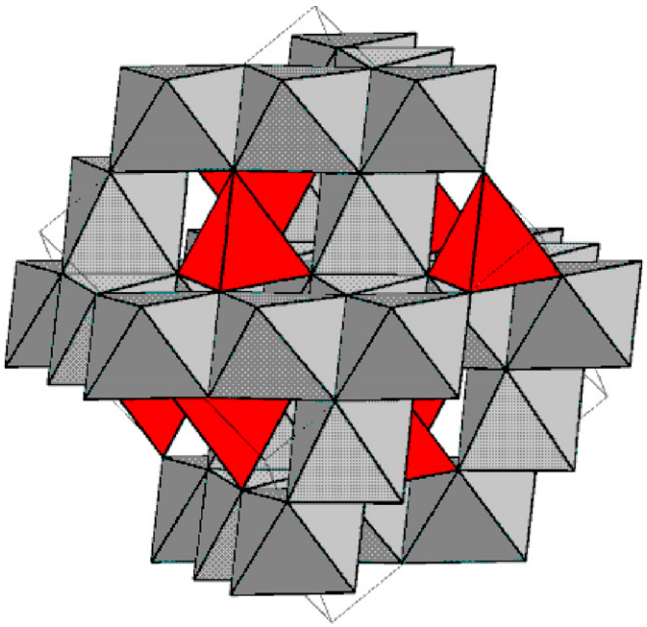

Fig. 5. Packing of the layers formed of octahedra and tetrahedral the spinel.

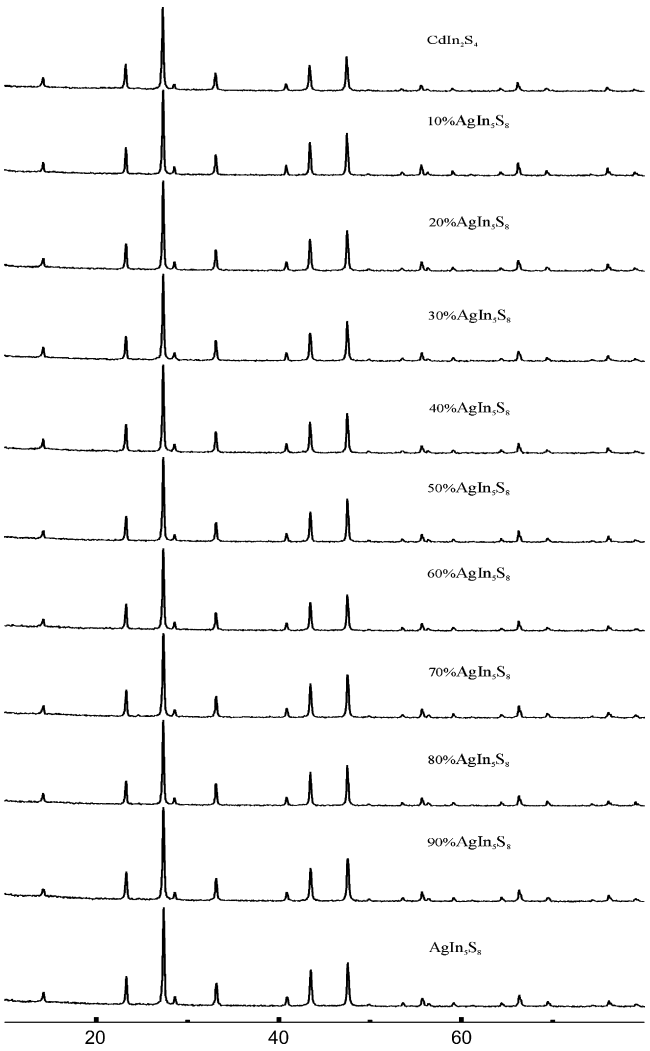

Fig. 6. Experimental diffraction patterns of the $AgIn_5S_8$–$CdIn_2S_4$ section.

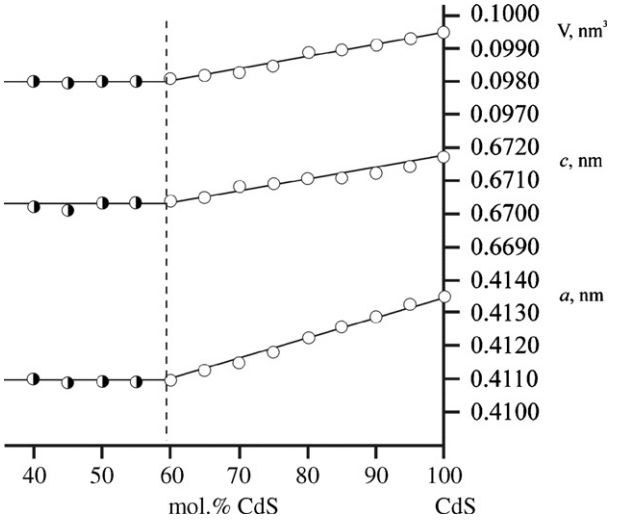

Fig. 7. The change of the unit cell parameters across the solid solution range of CdS in the $AgInS_2$–CdS system at 870 K.

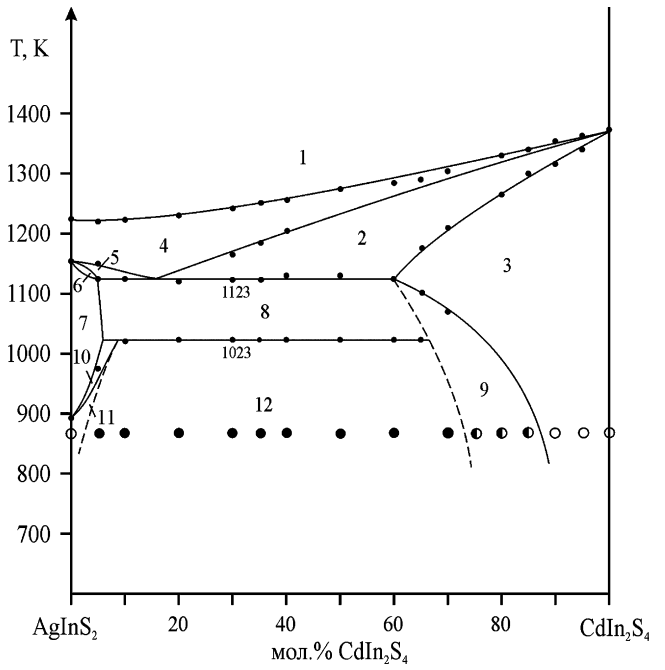

Fig. 8. Phase diagram of the $AgInS_2$–$CdIn_2S_4$ system: (1) L, (2) L + $AgIn_5S_8$ + $CdIn_2S_4$, (3) $CdIn_2S_4$, (4) L + $AgIn_5S_8$, (5) L + $AgIn_5S_8$ + β-$AgInS_2$, (6) $AgIn_5S_8$ + β-$AgInS_2$, (7) β-$AgInS_2$, (8) β-$AgInS_2$ + ε + CdS, (9) CdS + $CdIn_2S_4$, (10) α-$AgInS_2$ + β-$AgInS_2$, (11) α-$AgInS_2$, (12) α-$AgInS_2$ + ε + CdS.

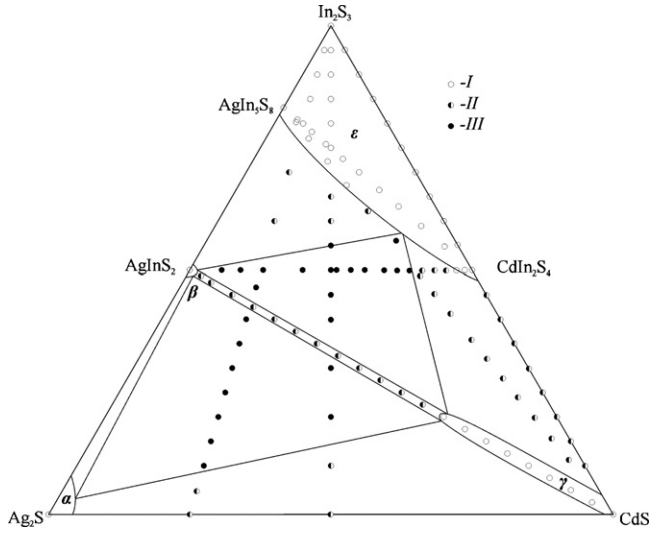

Fig. 9. Chemical and phase composition of alloys ((I) single-phase alloys, (II) two-phase alloys, and (III) three-phase alloys) and the isothermal section of the Ag_2S–In_2S_3–CdS system at 870 K.

nents, and thus the $AgIn_5S_8$–In_2S_3–$CdIn_2S_4$ sub-system is single-phase.

4. Conclusions

Phase equilibria in the quasi-ternary system Ag_2S–In_2S_3–CdS were investigated. The isothermal section of the system at 870 K was constructed. Large ranges of solid solubility of the binary compounds were discovered. The mechanism of the substitution in the solid solutions based on the initial compounds was determined.

References

[1] V.N. Tomashyk, V.I. Grytsiv, Phase Diagrams of the Systems Based on the Semiconductor Compounds AIIBVI, Naukova dumka, Kyiv, 1982.
[2] V.P. Sachanyuk, G.P. Gorgut, V.V. Atuchin, I.D. Olekseyuk, O.V. Parasyuk, J. Alloys Compd. 452 (2008) 348–358.
[3] V.B. Lazarev, Z.Z. Kish, Ye.Yu. Peresh, Ye.Ye. Semrad, Complex Chalcogenides in the A^{II}–B^{III}–C^{VI} Systems, Metallurgy, Moscow, 1993.
[4] G.D. Guseinov, G.B. Abdullaev, E.M. Kerimova, Mater. Res. Bull. 4 (1969) 807.
[5] R.J. Cava, F. Rcidinger, B.J. Wuensh, J. Solid State Chem. 31 (1980) 69.
[6] N.K. Abrikosov, V.F. Bakina, L.V. Poretskaya, et al., Semiconductor Chalcogenides and their Alloys, Nauka, Moscow, 1975.
[7] R. Diehl, R. Nitsche, Vapour, J. Cryst. Growth 20 (1973) 38.
[8] G. Delgado, A.J. Mora, C. Pineda, T. Tinoco, Mater. Res. Bull. 36 (2001) 2507.
[9] A.F. Qasrawi, N.M. Gasanly, Cryst. Res. Technol. 36 (2001) 457.
[10] H. Haeuseler, J. Solid State Chem. 29 (1979) 121.
[11] L.G. Akselrud, Yu.N. Grin', P.Yu. Zavalij, V.K. Pecharsky, V.S. Fundamensky, 12th Europ. Crystallographic Meet., Moscow Collected Abstracts Izv. Acad. Nauk SSSR 3, 1989.
[12] Martina Kerkhoff, Volkmar Leute, J. Alloys Compd. 385 (2004) 148–155.